Development 130, 1749-1758

doi:10.1242/dev.00397

A zone of frontonasal ectoderm regulates patterning and growth in the face

Diane Hu*, Ralph S. Marcucio* and Jill A. Helms†

Department of Orthopaedic Surgery, 533 Parnassus Avenue, Suite U-453, University of California at San Francisco, San Francisco, CA 94143, USA

*These authors contributed equally to this work
†Author for correspondence (e-mail: helms@itsa.ucsf.edu)

Accepted 14 January 2002

SUMMARY

A fundamental set of patterning genes may define the global organization of the craniofacial region. One of our goals has been to identify these basic patterning genes and understand how they regulate outgrowth of the frontonasal process, which gives rise to the mid and upper face. We identified a molecular boundary in the frontonasal process ectoderm, defined by the juxtaposed domains of *Fibroblast growth factor 8* and *Sonic hedgehog*, which presaged the initial site of frontonasal process outgrowth. Fate maps confirmed that this boundary region later demarcated the dorsoventral axis of the upper beak. Ectopic transplantation of the ectodermal boundary region activated a cascade of molecular events that reprogrammed the developmental fate of neural crest-derived mesenchyme, which resulted in duplications of upper and lower beak structures. We discuss these data in the context of boundary/morphogen models of patterning, and in view of the recent controversy regarding neural crest pre-patterning versus neural crest plasticity.

Key words: Craniofacial development, Patterning, *Fgf*, *Shh*, Neuroectoderm, Facial ectoderm, Neural crest, Frontonasal process, FNP, Branchial arch, Pharyngeal arch, Quail, Chick

INTRODUCTION

Almost 100 years of exploration into the mechanisms underlying morphogenesis has revealed that pattern formation is a remarkably conserved process, not only among phyla in the animal kingdom but also across disparate tissues and organs. From fields as diverse as mathematics, biophysics and biology, a unifying hypothesis has emerged that addresses how complex patterns can be generated in a dynamic environment (Dillon and Othmer, 1999; Gurdon and Bourillot, 2001; Meinhardt, 1983; Meinhardt, 1984; Wolpert, 1994; Wolpert, 1996). This convergent theory proposes that cells within a growing field sense and interpret multiple gradients of physical and chemical properties, then integrate this information and differentiate in a time- and location-dependent manner. These models have been used to describe, and possibly predict, how patterning and growth occurs in a number of embryonic tissues. We were interested in applying these same models to patterning and growth of the craniofacial complex.

There is an enormous literature indicating that the cranial neural crest, which gives rise to the connective tissues of the face, carries out cell-autonomous programs of differentiation. The rostrocaudal level of origin (Noden, 1983; Serbedzija et al., 1991), the expression of a 'Hox code' (Hunt et al., 1991b; Hunt et al., 1991c) and the timing of emigration from the neural tube (e.g. Artinger and Bronner-Fraser, 1992; Bronner-Fraser and Fraser, 1989; Richardson and Sieber-Blum, 1993) are thought to impart a 'pre-pattern' to neural crest populations. These data support the conclusion that craniofacial patterning is controlled by neural crest-derived mesenchyme (reviewed by Dorsky et al., 2000).

However, abundant data underscore the significance of environmental signals in determining cell fate. The transplantation (Baker et al., 1997; Couly et al., 1998; Hunt et al., 1998; Schneider, 1999) or ablation (Raible and Eisen, 1996) of neural crest, the transplantation or ablation of local signaling centers (Couly et al., 2002), the alteration of gene expression patterns by electroporation (Creuzet et al., 2002; Grammatopoulos et al., 2000), in vitro co-culture experiments (Tyler and Hall, 1977) and experiments in which the addition of signaling molecules transform cell identity (Lee et al., 2001) all indicate that neural crest cells retain a considerable degree of plasticity. These data support the conclusion that local environmental signals regulate craniofacial patterning by eliciting a range of responses from an uncommitted population of neural crest.

We find the balance between neural crest pre-determination and plasticity particularly compelling, and have pursued this issue in the context of craniofacial morphogenesis. Our investigation focuses on the mechanisms that regulate patterning and growth of the frontonasal process (FNP), which gives rise to the mid and upper face, and (in birds) contributes to the upper beak. Bird beaks exhibit an astonishingly variable morphology, ranging from that of the Snail-Eating Coua to the Roseate Spoonbill and variations in beak shape have been closely associated with adaptive radiation into new niches (Darwin, 1859). Both aspects make the question of how the beak attains its pattern a particularly enticing problem to

address. Our first postulation was that changes in beak morphology could result from subtle alterations in epithelial-mesenchymal interactions in the FNP. Thus, we began our studies by examining the extent to which ectodermal signals controlled patterning and growth of the FNP.

MATERIALS AND METHODS

Fate mapping the FNP

Replication-competent and replication-incompetent retroviruses encoding alkaline phosphatase (RCAS-AP and RIS-AP, respectively) were produced as described (Fekete and Cepko, 1993). Briefly, DF-1 cells were transfected with proviral DNA and expanded in Dulbecco's Minimum Essential Medium (DMEM) supplemented with 10% FBS; cells were passaged twice. Viruses were harvested over 3 consecutive days from confluent cultures grown in low serum conditions (e.g. 1% FBS). Viral supernatants were filtered to remove cells and centrifuged at 87,275 ***g*** for 3 hours to concentrate virions. The supernatants were discarded, viral pellets were re-suspended in low serum culture medium, and 20 μl aliquots were frozen at –80°C. One microliter of 0.02% Fast Green was added to each 10 μl viral supernatant to aid in visualization during injection. The virus-dye solution was drawn up into a pulled borosilicate glass capillary pipette (OD=1.0 mm; ID=0.50 mm; Sutter Instrument, Novato, CA), attached to a KITE-R micromanipulator (World Precision Instruments, Sarasota, FL), and injected using a PV830 Pneumatic Picopump (World Precision Instruments, Sarasota, FL). Virus was injected into the FNP of stage 20 chick embryos; embryos were fixed in 4% paraformaldehyde (PFA) in phosphate buffered saline (PBS) after 48 hours, or after 7 days. Endogenous alkaline phosphatases were inactivated by incubation in PBS at 65°C for 30 minutes. Infected cells were visualized by washing embryos three times in PBS and incubating in BM-purple (Roche) until a blue reaction product was visible.

In situ hybridization

In situ hybridization was performed on whole avian embryos and paraffin wax-embedded sections as described (Albrecht et al., 1997). Subclones of *Shh*, *Ptc1*, *Gli1*, *Islet1*, *Lfng*, *Rfng*, *Fgf8*, *Fgf10*, *Barx1*, *FgfR1-3*, *AP2*, *Bmp2*, *Bmp4*, *Bmp5*, *Bmp6*, *Bmp7*, *BmpR1a*, *BmpR2b*, *Noggin*, *Gremlin*, *Follistatin*, *DAN*, *Wnt4*, *Wnt6*, *Wnt7a*, *Wnt7b*, *Wnt13*, *Wnt14*, β-*catenin*, *Tbx2*, *Tbx3*, *Dlx1*, *Engrailed1*, *Engrailed2*, *Frzb1*, *LEF*, *Notch*, *Delta* and *Serrate* were linearized to transcribe either ^{35}S-labeled or digoxygenin-labeled antisense riboprobes. The expression patterns of all of these genes were examined at multiple stages during craniofacial development; a subset of expression patterns is shown here. For ^{35}S-labeled riboprobes, the hybridization signal was pseudo-colored using Adobe Photoshop, then superimposed onto an image of the tissue stained with Hoechst nuclear stain (Sigma). Whole-mount in situ hybridization was performed as described (Albrecht et al., 1997).

Graft preparation and transplantation

Tissue grafts consisting of FNP ectoderm and mesenchyme were harvested from stage 20 (Hamburger and Hamilton, 1951) quail embryos using sharpened tungsten needles (illustrated in Fig. 2A). The FNP tissues were placed in DMEM digested with Dispase (2.4 units/ml, on ice for 20 minutes) to facilitate separation of ectoderm from mesenchyme, then washed in DMEM containing 1% BSA to stop the digestion. FNP ectoderm grafts, measuring 0.5-0.8 mm in height by 1.0-1.2 mm in width, and free of adherent mesenchyme, were transferred into DMEM containing Neutral Red (23°C, 2 minutes), which was added to facilitate visualization of the graft when transferred to the host.

Stage 25 chick embryos served as hosts. Embryos were positioned in the egg to gain access to the facial primordia, and the graft site was prepared by removing FNP ectoderm from the dorsal midline with tungsten needles; care was taken to avoid excessive disruption of underlying mesenchyme. The donor grafts were positioned in the dorsal region of the host FNP and secured in place using glass pins (Fig. 2A). Chimeric embryos were incubated for 12, 24, 48 hours, and for 7 and 10 days for molecular, cellular, histological and morphological analyses.

Immunohistochemistry

To detect quail cells, chimeric embryos were removed 12 and 24 hours, and 7 days after graft transplantation, fixed in Serra's, paraffin wax embedded, and cut into 10 μm sagittal sections. Immunodetection of quail cells used QCPN, the quail-specific monoclonal antibody (Developmental Studies Hybridoma Bank), followed by incubation with a second antibody conjugated to Horseradish peroxidase (HRP). Diaminobenzidine (DAB, Sigma) was used to detect HRP. Sections were counterstained with Fast Green FCF (Fisher) and imaged using brightfield optics.

Bead implantations

Heparin sulfate beads (200-250 μm diameter; BioRad) were soaked in a solution containing Fgf2 protein (400 μg/ml; R & D Systems), at 37°C for 1 hour. Affi-Gel Blue beads (50-100 mesh, 200-250 μm diameter; BioRad) were soaked in recombinant Shh-N protein (400 μg/ml in PBS with 0.1% bovine serum albumin; Ontogeny) at 37°C for 1 hour. Fgf2 beads, Shh-N beads, or a combination of both beads were implanted into the dorsal FNP of stage 25 embryos, underneath the host ectoderm. When a bead and a graft were combined, the graft was positioned, stabilized with glass pins in three corners, and then the bead was placed beneath the edge of the graft. The fourth corner of the graft was secured with a glass pin as described. Seven days later, embryos were examined for morphological alterations by gross examination and histology.

Histology

Embryos were sacrificed at stage 36; their heads were fixed in 4% PFA overnight at 4°C, dehydrated and embedded in paraffin wax. Heads were cut into 10 μm sagittal sections, which were stained with Milligan's Trichrome (Presnell and Schreibman, 1997).

RESULTS

Defining the dorsoventral axis of the upper beak

Our first objective was to understand the cellular movements that create the three-dimensional organization of the upper beak (see also McGonnell et al., 1998). Using RCAS-AP and RIS-AP, we followed the fate of small groups of ectodermal cells in the stage 20 FNP (Fig. 1). Both retroviruses produced similar results, and showed that infection of cells in the dorsolateral FNP (Fig. 1A, site B) resulted in AP staining in proximal regions of the upper beak (*n*=10, Fig. 1B). Of particular interest to us was the result of injections performed within a narrow band of ectoderm extending, in a mediolateral direction, across the FNP (Fig. 1A, sites C,D). These injections resulted in AP staining along a margin of the upper beak that separated the dorsal surface from the ventral (Fig. 1C,D). We focused on this area, and found that when cells at the midline of this ectodermal band were infected, AP staining was detected at the very tip of the beak (*n*=8, Fig. 1D), while infection of more lateral cells produced staining along the proximal edges (*n*=10, Fig. 1C). Infection of cells below the base of the FNP (Fig. 1A, site E) resulted in AP staining on the ventral surface of the beak (*n*=5, Fig. 1E). Thus, our fate

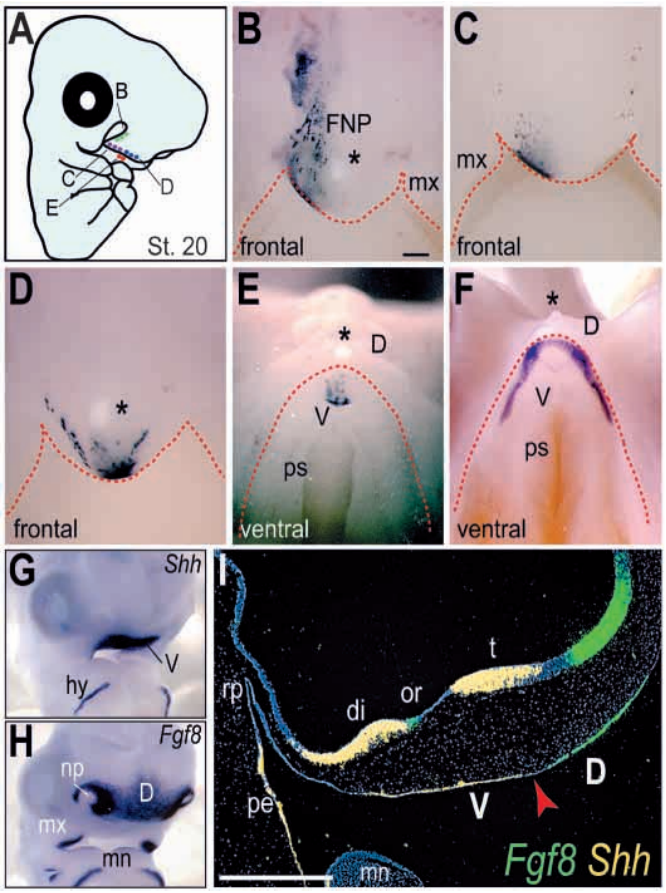

Fig. 1. Defining morphogenetic movements and molecular boundaries in the upper beak. (A) A stage 20 embryo illustrating four primary sites of retroviral application. Broken red lines trace the border of the FNP and maxillary processes, and colored dots correspond to injections sites shown in B-E. (B) Infected cells were visualized after histochemical detection of alkaline phosphatase activity (blue precipitate). A frontal view of a stage 30 embryo showed that injections at site B labeled a patch of ectodermal cells that extended along the dorsal aspect of the FNP. The egg tooth is indicated by an asterisk. (C) Frontal view of a stage 28 embryo showed that injections at site C labeled ectodermal cells on the dorsal margin of the upper beak. (D) Frontal view of a stage 30 embryo showed that injections at site D produced labeled cells that resided along the dorsal margin of the upper beak. (E) Ventral view of a stage 30 upper beak, which demonstrated that injections at site E resulted in labeled cells along the midline of the ventral upper beak. The broken red line indicates the dorsoventral boundary, (F) which was demarcated by the *Shh* expression domain. (G) Whole-mount in situ hybridization demonstrated that by stage 20, *Shh* was expressed in ventral FNP ectoderm (V); transcripts were also evident in hyoid arch (hy) ectoderm. (H) Also at stage 20, *Fgf8* was expressed in dorsal FNP ectoderm (D); transcripts were detectable around the nasal pit (np), in the maxilla (mx) and mandible (mn), and on the posterior aspect of the hyoid arch. (I) The juxtaposed (red arrowhead), but not overlapping boundary of *Fgf8* (transcripts pseudocolored green) in dorsal FNP (D) and *Shh* (yellow) in ventral ectoderm (V) was confirmed by section in situ hybridization. ps, palatal shelf; pe, pharyngeal endoderm; rp, Rathke's pouch; di, diencephalon; or, optic recess; t, telencephalon. Scale bar: in B, 1 mm for B-F; in I, 0.5 mm.

maps suggested that a dorsoventral axis was established in the FNP prior to the initiation of outgrowth.

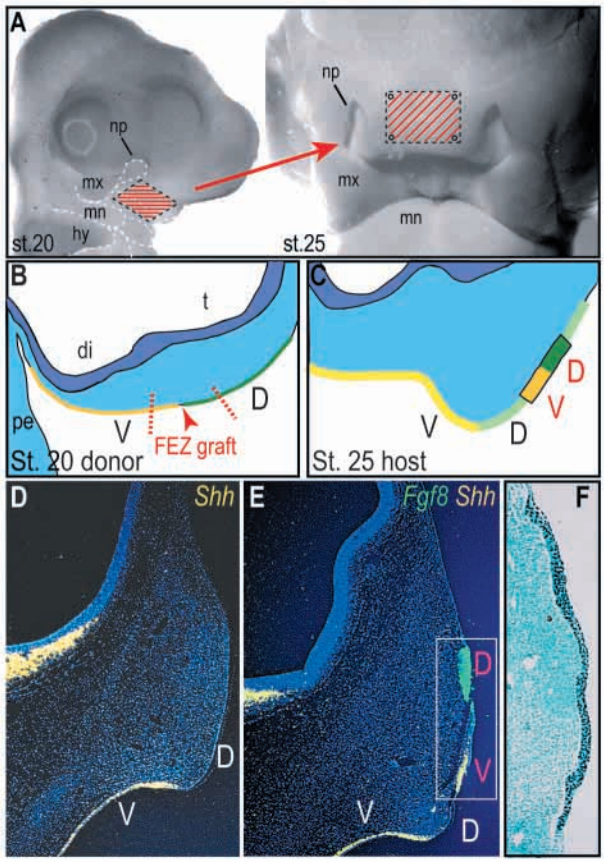

Fig. 2. Transplantation of the FEZ creates an ectopic *Fgf8/Shh* boundary. (A) A region of stage 20 FNP ectoderm measuring 0.5-0.8 mm by 1.0-1.2 mm in width (indicated by the red striped box) was transplanted onto the dorsal FNP (D) of a stage 25 chick embryo and pinned into place. (B) Lateral schematic view of the FEZ donor site (broken red lines indicate cut sites). FEZ grafts encompassed the *Fgf8* (green) ventral *Shh* (yellow) junction (indicated by a red arrow). (C) Lateral schematic view of the FEZ graft site in a stage 25 host FNP. The quail-derived FEZ graft is indicated by a darker green (dorsal) and a darker yellow (ventral) domain, and by red letters. Twelve hours after transplantation, (D) *Shh* expression persisted in the ventral FNP ectoderm (V) of stage-matched, unoperated embryos. (E) Ectopic *Fgf8* and *Shh* in the dorsal FNP of chimeric embryos confirmed that the FEZ (red D,V) was appropriately positioned in the host FNP. (F) Higher magnification of the boxed region in E showed that only QCPN-positive quail ectoderm was transplanted. ps, palatal shelf; pe, pharyngeal endoderm; rp, Rathke's pouch; di, diencephalon; or, optic recess; t, telencephalon.

Our next objective was to identify genes whose expression patterns implicated them in the establishment of a putative dorsoventral FNP axis. Two obvious candidates were *Fgf8* and *Shh* because of their capacity to mediate axis specification and patterning in other developmental systems (Laufer et al., 1994; Ye et al., 1998). Using whole-mount in situ hybridization, we found that in the FNP, *Shh* transcripts were restricted to a ventral region, while *Fgf8* transcripts were limited to a dorsal region (Fig. 1G,H). To find out if these domains were mutually exclusive or overlapped to some degree, we compared the *Fgf8* and *Shh* expression patterns on adjacent tissue sections using sectioned in situ hybridization. We found that the ventralmost extent of *Fgf8* abutted (but did not overlap with) the dorsalmost

site of *Shh* (*n*=10, Fig. 1I). We examined 23 other candidate genes (see Materials and Methods for a complete list) and none exhibited the same restricted pattern of expression at this early stage of development (R.S.M. and J.A.H., unpublished). Thus, our molecular analyses indicated that the *Fgf8*/*Shh* expression boundary, which corresponded to the fate-mapped dorsoventral margin, presaged the site of proximodistal growth of the FNP. Henceforth, we refer to the stage 20 *Fgf8*/*Shh* expression boundary as the frontonasal ectodermal zone (FEZ).

Transplantation of the FEZ alters dorsoventral patterning of the FNP

We suspected that the FEZ controlled aspects of dorsoventral patterning in the FNP, and developed a transplantation strategy to test this possibility. In the first set of experiments, we grafted the FEZ from a quail embryo onto the dorsal FNP of a stage 25 chick host (Fig. 2A-C). We performed these heterochronic transplants because a stage 25 FNP is sufficiently large to accommodate a FEZ graft without disrupting or interfering with ectoderm at the tip of the FNP. In our first experiment, the orientation of the FEZ graft was maintained in the host (Fig. 2B,C). We collected chimeric embryos and unoperated, stage-matched controls for the first analyses 12 hours after transplantation. We used in situ hybridization to demonstrate that the graft was appropriately positioned in the host, and continued to express *Fgf8* and *Shh* in its ectopic position (*n*=7, Fig. 2D,E). We used QCPN immunostaining to confirm that the graft was composed entirely of ectodermal cells from the quail donor, with no adherent mesenchyme (*n*=7, Fig. 2F).

Within 12 hours the FEZ graft induced cell proliferation and re-specified gene expression patterns in the underlying dorsal FNP mesenchyme. By 24 hours, these altered expression patterns were even more pronounced, and the first morphological evidence of an ectopic outgrowth was observed (*n*=15, Fig. 3). The changes in gene expression were consistent with the orientation of the graft; for example, *Shh* is normally restricted to ventral FNP ectoderm (Fig. 3A,D); when the FEZ was positioned in its original dorsoventral orientation (i.e., no rotation), a *Shh*-off/*Shh*-on/*Shh*-off/*Shh*-on pattern (from dorsal to ventral) was created in the chimeric ectoderm (*n*=10, Fig. 3B,E). Ectopic *Ptc1* and *Gli1* in the mesenchyme reflected the location of *Shh* in the ectoderm being induced beneath the *Shh*-positive regions and downregulated beneath the *Shh*-negative

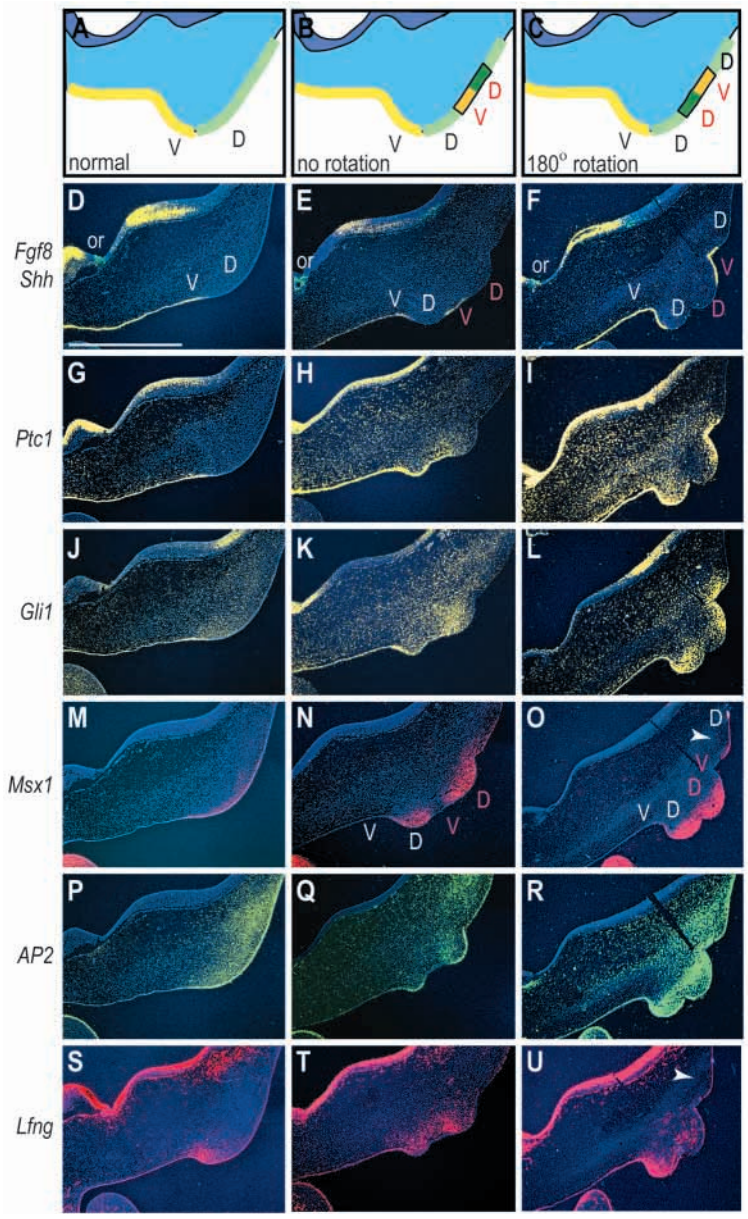

Fig. 3. Changes in gene expression patterns correspond to FEZ orientation. (A) Schematic lateral view of a stage 25 host FNP, indicating dorsal (green) and ventral (yellow) domains corresponding to sections shown in D,G,J,M,P,S. (B) Schematic view of a quail FEZ graft (dark green, dark yellow, red D,V) positioned on the dorsal surface of a stage 25 chick host FNP corresponding to sections shown in E,H,K,N,Q,T. (C) Schematic view of a FEZ graft that has been rotated 180° (red V,D) corresponding to sections shown in F,I,L,O,R,U. (D) In unoperated embryos, *Shh* (yellow) was restricted to ventral FNP ectoderm (V); *Fgf8* was already down regulated in dorsal FNP ectoderm (D) but transcripts were still detectable in the optic recess (or). (E,F) Twenty-four hours after transplantation, *Shh* was detected in the ventral FEZ (red V) as well as in its endogenous, ventral domain (white V). *Fgf8* was no longer detectable in the dorsal FEZ (red D). (G) *Ptc1* transcripts were detected in ventral ectoderm and throughout FNP mesenchyme. (H,I) *Ptc1* was ectopically induced in FNP mesenchyme beneath the ventral region of the graft. (J) *Gli1* was expressed in ventral ectoderm and at low levels throughout FNP mesenchyme. (K,L) *Gli1* was ectopically induced in mesenchyme beneath the ventral FEZ. (M) *Msx1* was expressed in dorsal ectoderm and mesenchyme, corresponding to the site of outgrowth. (N,O) *Msx1* was repressed beneath the ventral, and induced beneath the dorsal, FEZ; a small ectodermal patch of *Msx1* was evident in dorsal host ectoderm but was absent in underlying mesenchyme (O, arrowhead). (P) *AP2* was strongly expressed throughout the dorsal ectoderm and mesenchyme. (Q,R) *AP2* transcripts were abundant beneath both the dorsal and ventral FEZ. (S) *Lfng* was expressed at low levels throughout the ectoderm and localized to the mesenchyme at the site of outgrowth. (T,U) The endogenous mesenchymal expression of *Lfng* was up regulated adjacent to the graft, as well as in the mesenchyme beneath the ventral graft, but was missing from the dorsal mesenchyme (arrowhead). Scale bars: 1 mm.

regions (Fig. 3H,K). We also analyzed chimeric and control embryos for *Fgf8* expression. Although *Fgf8* continued to be expressed in the optic recess (Fig. 3D-F), it was downregulated in the host FNP ectoderm and the FEZ graft by this stage. Nonetheless, downstream targets of Fgf signaling, including *Msx1* and *AP2*, were upregulated under the previously *Fgf8*-positive dorsal part of the FEZ graft and downregulated under the *Fgf8*-negative ventral region of the FEZ (Fig. 4M,N,P,Q). Other genes, such as *Lfng* and most of the Bmp genes, were upregulated in FNP mesenchyme underneath the graft (Fig. 3S,T, and data not shown). When the graft was rotated 180° (Fig. 3C), we found the predicted reversal in the *Shh* pattern (e.g. *Shh*-off/*Shh*-on/*Shh*-off/*Shh*-on; Fig. 3F). Correspondingly, *Ptc1* and *Gli1* were upregulated in the mesenchyme under the ventral *Shh* domains (Fig. 3I,L) while dorsal genes such as *Msx1* and *Lfng* were upregulated under dorsal regions of the FEZ graft and repressed under ventral regions (Fig. 3O,U). Neither *Msx1* nor *Lfng* was expressed in the dorsal-most mesenchyme (Fig. 3O,U, arrowheads). The ability to re-specify gene expression in FNP mesenchyme was not shared by other ectodermal grafts, including stage 20 dorsal facial ectoderm (n=6) and stage 20 flank ectoderm (n=6).

The FEZ also induces FNP outgrowth

Thus far, our results indicated that ectodermal signals from the FEZ could override a molecular 'pre-pattern' in neural crest-derived mesenchyme. To determine if this molecular re-programming resulted in alterations in facial patterning, we repeated the grafting experiments and examined control and chimeric embryos at stage 36 (Fig. 4). By this time, the upper beak exhibits unequivocal dorsal and ventral features such as the egg tooth, a transitory cornified thickening of the dorsal epidermis located near the tip of the upper beak, the premaxillary bone, which lies immediately underneath the egg tooth, and the cartilaginous prenasal process, which is the equivalent of the prenasal septum in mammals and is

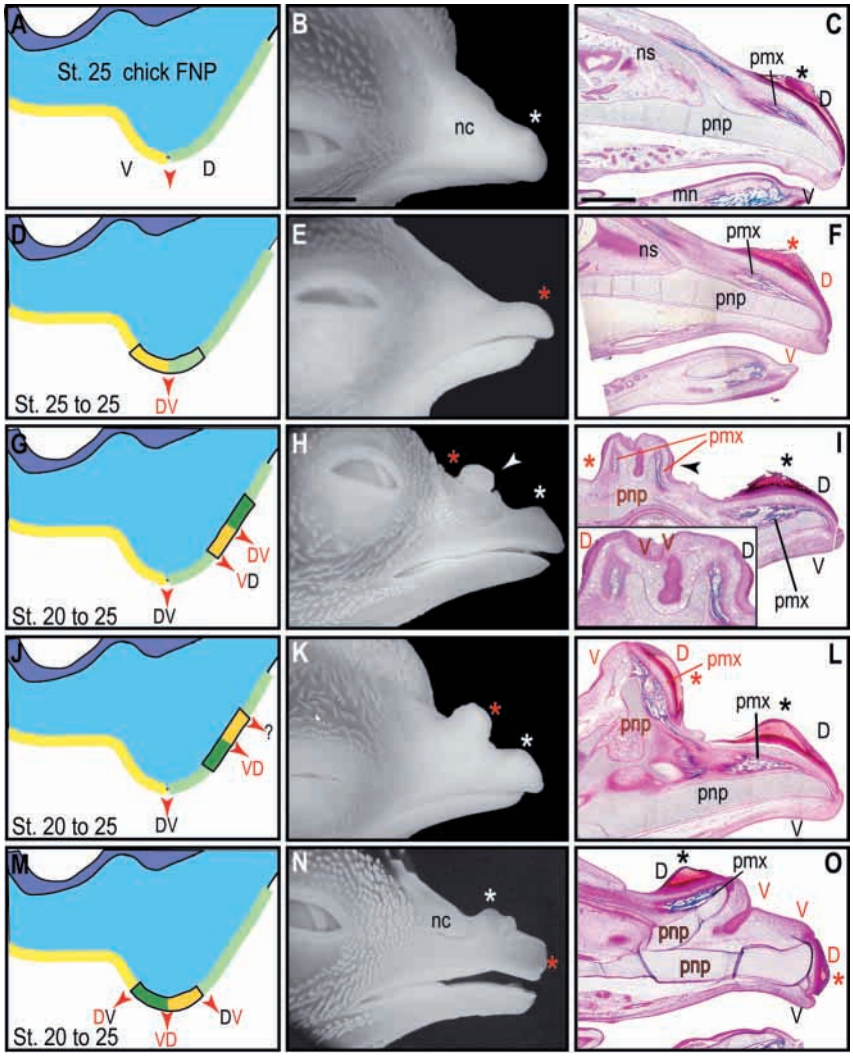

Fig. 4. The FEZ induces outgrowth of an ectopic beak that exhibits dorsoventral polarity. (A) Schematic view of a stage 25 host FNP, indicating that the intersection of the dorsal (green) and ventral (yellow) compartments was the site of outgrowth (red arrow). (B) By stage 36, an egg tooth (*) was evident on the dorsal upper beak, while the ventral surface has no ectodermal elaborations. (C) Sagittal trichrome-stained section through the embryo shown in B demonstrates the dorsoventral relationships among structures in the upper beak. The egg tooth (asterisk) is located on the dorsal surface; beneath it is the premaxillary bone (pmx), and below this is the prenasal process (pnp). The ventral surface of the upper beak (V) lacks any elaborated ectodermal appendages. (D) Schematic view of a stage 25 host after transplantation of quail stage 25 FNP ectoderm (red DV). (E,F) This isotopic transplantation had no effect on facial morphology, despite the fact that the graft was derived from quail. (G) Schematic view of stage 25 host after FEZ transplantation. The graft is positioned in the normal, dorsoventral orientation. The expected outgrowths (arrowheads), with their predicted dorsoventral polarity are indicated. (H) This grafting scenario resulted in an outgrowth from the proximal region of the upper beak and contained two egg teeth. The autochthonous egg tooth (arrowhead) appears normally positioned. (I) The ectopic beak comprised two egg teeth (red asterisk and arrowhead) located above two premaxillae (red pmx) each surrounding a prenasal process (red pnp). These relationships indicated that the ectopic beak had dorsal-ventral/ventral-dorsal polarity (DVVD). The autochthonous beak contained an egg tooth (black asterisk), the premaxilla (black pmx), and the prenasal process (black pnp, dorsal ventral indicated by D and V). (J) Schematic view of stage A 25 host after transplantation of a rotated FEZ. The expected outgrowths (arrowheads), with their predicted dorsoventral polarity are indicated. (K) The ectopic upper beak had a single egg tooth (red asterisk). (L) The presence of a single egg tooth (red asterisk), a single premaxilla (red pmx), and a single prenasal process (red pnp) indicated the ectopic structure had ventral/dorsal polarity. (M) Schematic view of a stage 25 host after isotopic transplantation of a rotated FEZ. The expected outgrowths (arrows) and their predicted dorsoventral polarity are indicated. (N) An ectopic structure was evident and, (O) histological analysis indicated the presence of two egg teeth, a dorsal premaxilla and two prenasal processes. The relative positions of these structures indicated a DV/VDV polarity to the beaks. Scale bars: 1 mm.

positioned ventral to the premaxillary bone (Fig. 4). As a control, we replaced stage 25 chick FNP ectoderm with stage 25 quail FNP ectoderm (Fig. 4D-F). The grafted embryos were indistinguishable from their unoperated, stage-matched controls, indicating that the surgery alone did not alter facial morphology (*n*=8; Fig. 4E,F). Likewise, when stage 25 facial ectoderm was grafted to the dorsal FNP of a host embryo, the chimeric embryos resembled their unoperated controls. This finding indicated that a stage 25 ectoderm graft did not alter facial morphology (*n*=6, data not shown).

In contrast to a stage 25 FNP ectoderm graft, a FEZ graft dramatically altered facial pattern. In most cases (36/38), an enormous outgrowth was observed at the site of graft placement (Fig. 4H,K,N). We used the spatial relationships among the egg tooth, the premaxillary bone, and the prenasal process to define the dorsoventral axis of the structures induced by the FEZ. By these criteria, two ectopic upper beaks formed (Fig. 4H,I). These ectopic structures were mirror-image (e.g. dorsal-ventral/ventral-dorsal) duplications of one another; the autochthonous beak maintained its normal dorsoventral polarity (Fig. 4I). We annotated this pattern as *DVVD*/DV to reflect the polarity of the structures induced by the quail FEZ (in italics) and the autochthonous upper beak. The assignment of a *DVVD* pattern to the ectopic structures was further supported by molecular analyses performed 12 and 24 hours after grafting, which showed an *Msx1/Shh/Msx1/Shh* expression pattern in the FNP ectoderm (*n*=10; Fig. 3 and data not shown). Thus, the FEZ induced the formation of two new dorsoventral boundaries within the FNP, and the outgrowth of two ectopic upper beak structures, whose own dorsoventral polarity was determined by the graft.

Based on these data, we hypothesized that juxtaposing dorsal and ventral ectodermal domains would be sufficient to stimulate the outgrowth of beak structures. We tested this hypothesis by rotating the FEZ 180° prior to grafting, which positioned the ventral (*Shh*-positive) domain of the graft adjacent to the dorsal (*Fgf8/Msx1*-positive) domain of the host, and the dorsal domain of the graft adjacent to the ventral domain of the host (Fig. 4J). As predicted, the ensuing molecular pattern in the ectoderm was *Msx1-Shh-Msx1-Shh* (*n*=10; Fig. 3). Only one ectopic outgrowth was produced, which was a mirror-image duplication of the autochthonous beak (*VD*/DV; 7/7 cases, Fig. 4K,L). We did not detect the predicted third upper beak (Fig. 4J, question mark), presumably because of the failure to reprogram the dorsalmost mesenchyme (see Fig. 3O,U, arrows).

To explore further if juxtaposing dorsal and ventral domains was sufficient to induce outgrowth, we transplanted stage 20 ventral ectoderm to the dorsal surface of a stage 25 host FNP. By doing so, we theoretically created two new sites where dorsal and ventral tissues were apposed, and where outgrowth should ensue if our initial hypothesis was correct. We confirmed that the grafts comprised only ventral ectoderm (*n*=12, in situ hybridization data not shown), and examined chimeric embryos for morphological and histological alterations 7 days later. Ventral grafts were unable to induce FNP alterations analogous to those caused by the FEZ graft (*n*=14; data not shown). Taken together, these data show that FNP outgrowth does not necessarily result from the juxtaposition of dorsal and ventral FNP ectoderm. Instead, our data indicate that FNP outgrowth requires other signals unique to the FEZ domain, or unique to the mesenchyme underlying the FEZ.

The FEZ can override an existing FNP pattern

We explored the extent to which a FEZ graft could alter the endogenous FNP pattern. First, we confirmed that removing stage 25 facial ectoderm truncated the growth of the upper beak at the level of the nasal capsule (*n*=10, data not shown) (see Hu and Helms, 1999). Next, we replaced FNP ectoderm with a FEZ graft, which had been rotated 180° prior to transplantation. This rotation resulted in the juxtaposition of ventral FEZ with dorsal host ectoderm and dorsal FEZ with ventral host ectoderm (Fig. 4M). By rotating the FEZ, we were able to ascertain the extent to which neural crest-derived mesenchyme was plastic versus pre-specified, with regards to dorsoventral pattern. Two beaks were evident as a result of the grafting (Fig. 4N,O). The first beak, in the ectopic location, had a DV pattern. The second beak, in the autochthonous location, lacked a (dorsal) premaxillary bone; in addition, the egg tooth, which is a dorsal specialization, was now located at the apex of the beak. Furthermore, the prenasal process was

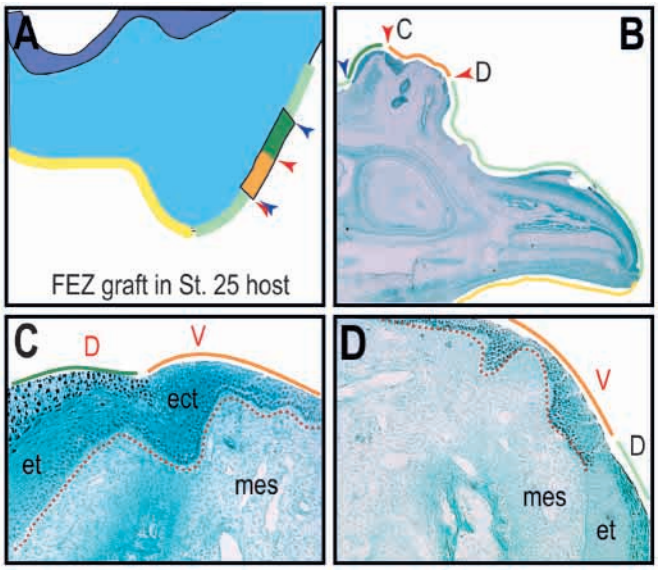

Fig. 5. QCPN staining indicates that FNP outgrowths occur at dorsoventral compartment boundaries. (A) Schematic view of a stage 25 host FNP illustrating two types of boundaries. One type of boundary is created between quail and chick tissues (i.e. a heterospecific junction); these are indicated with blue arrows. Another type of boundary is created by the juxtaposition of dorsal and ventral ectoderm; we refer to these as dorsoventral compartment boundaries and they are indicated with red arrowheads. (B) QCPN immunostaining identified ectodermal domains comprised of quail FEZ and chick FNP ectoderm. The colored lines indicate both the polarity and source of the ectoderm. Dorsal ectoderm is green and ventral is yellow, and quail tissues are indicated with darker lines. C, the transplanted FEZ; D, a new FEZ created by the juxtaposition of chick dorsal and quail ventral ectoderm (shown at higher magnification in C,D. Note that the junction of chick dorsal and quail dorsal ectoderm (blue arrowhead) did not result in an outgrowth. (C) Quail-positive ectoderm spanned the dorsoventral boundary of the ectopic outgrowth (quail nuclei are black; the broken red line demarcates the epithelial-mesenchymal interface). (D) The juxtaposition of quail ventral ectoderm and chick dorsal domains resulted in the creation of a chimeric FEZ. mes, mesenchyme; et, egg tooth.

symmetrically shaped rather than exhibiting a typically convex dorsal surface and concave ventral surface. Thus, we ascribed a VDV pattern to the second beak (Fig. 4N,O). These results demonstrated that the FEZ graft could re-program the fate of FNP neural crest-derived mesenchyme, even at a very late stage in facial development.

FNP outgrowths occur at dorsoventral compartment boundaries

The immunohistochemical localization of quail cells had previously established that FEZ grafts consisted of ectoderm with no adherent mesenchyme (Fig. 2F). We now used QCPN immunostaining to demonstrate conclusively that the dorsoventral molecular boundaries corresponded to the initiation sites of FNP outgrowth. Boundaries resulting from the juxtaposition of two dorsal domains (e.g. Fig. 5A, blue arrow) were not associated with sites of outgrowth and were instead characterized by the seamless continuity of chimeric ectoderm (Fig. 5B). The juxtaposition of quail ventral ectoderm and chick dorsal ectoderm created a chimeric FEZ (Fig. 5A), which resulted in an ectopic outgrowth (Fig. 5D). In only one location, where ventral FEZ abutted the dorsalmost region of the FNP, did we fail to observe a predicted outgrowth (Fig. 4J, question mark). The reasons for this are unclear, but may be related to our previous observation that *Msx1* and *Lfng* were not induced in this dorsalmost mesenchyme as they were in FEZ-associated mesenchyme (Fig. 3O,U). Nonetheless, the immunohistochemical data confirmed that unlike other regions of FNP ectoderm, dorsal and ventral regions of the FEZ were sufficient to induce FNP outgrowth.

An ectopic FEZ re-patterns the mandibular, but not the hyoid, arch

In our next series of experiments we tested the plasticity of neural crest-derived mesenchyme in the first and second pharyngeal arches. When the FEZ was transplanted to a stage 25 mandible, an ectopic skeletal element formed (Fig. 6A-C), which appeared to result from the bifurcation of Meckel's cartilage (Fig. 6D, broken white line). The ectopic cartilaginous rod was surrounded by bone at its distal extent, which resembled the mandibular symphysis (Fig. 6E). There was no evidence of an egg tooth on the distal tip of the outgrowth (Fig. 6A-C), providing further support for our interpretation that the structure was an ectopic distal mandible. We performed a series of in situ hybridization analyses and determined that *Fgf8* and *Shh* expression were maintained in the FEZ graft for at least 24 hours (Fig. 6F) and caused an expansion of *Barx1*, *Ptc1*, *Gli1*, *Bmp2* and *Msx1*, and to a lesser extent *LFng*, into the posterior region of the mandibular arch (data not shown). Thus, the FEZ had the ability to re-program the molecular and ultimately, cellular fate of first pharyngeal arch mesenchyme.

Transplantation of the FEZ to the second pharyngeal (hyoid) arch produced a completely different response: the graft did not induce alterations in soft tissue (Fig. 7A,B) or hard tissue morphology (Fig. 7C,D). *Fgf8* and *Shh* were not maintained in the graft (*n*=4; data not shown), and *HoxA2*, which is normally expressed in the hyoid arch ectoderm and mesenchyme (Hunt et al., 1991a) was unaffected by FEZ transplantation (*n*=4; data not shown). From these data, we conclude that signals from the FEZ were able to alter the molecular and cellular fate of neural crest in the first pharyngeal arch and FNP. By contrast, the FEZ was unable to alter the fate of neural crest cells in the second pharyngeal arch.

Fgf2 can restore FEZ activity to stage 25 FNP ectoderm

Stage 25 FNP ectoderm does not exhibit the same capacity to re-pattern the FNP as does the FEZ. One molecular difference between stage 25 FNP ectoderm and stage 20 FEZ is that *Fgf8* is not expressed in the older ectoderm. We therefore tested if a stage 25 FNP ectoderm graft, combined with an Fgf2 bead, could recapitulate the patterning function of a FEZ graft. The resulting chimeric embryos exhibited a duplication of the upper beak structures (Fig. 8A-C) similar to those induced by the FEZ (see Figs 4, 5). Although the ectopic premaxillary bone and prenasal process were smaller than the FEZ-induced equivalents, the upper beak clearly exhibited a *DV*/DV pattern and thus a duplicated dorsoventral axis.

Given the ability of the Fgf2/stage 25 FNP graft combination to reconstitute the patterning effects of the FEZ, we next tested if Fgf and Shh proteins by themselves could mimic a FEZ graft. We positioned Shh-N beads underneath stage 25 FNP ectoderm in the same *Fgf8*-positive region as the FEZ graft had been

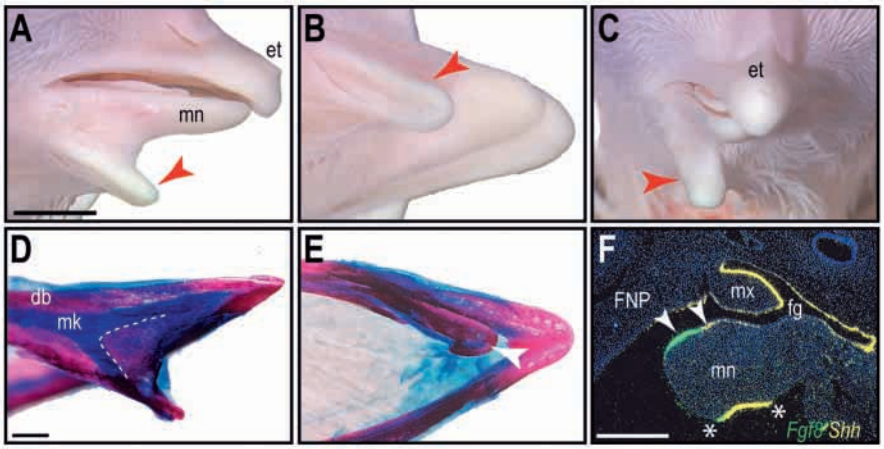

Fig. 6. The FEZ graft induces an ectopic outgrowth in the mandible. (A) Lateral, (B) ventral and (C) frontal views of chimeric embryos with ectopic outgrowths (red arrow) that formed 7 days after transplantation. No ectodermal appendages, such as the egg tooth (et), were present on the outgrowths. (D,E) Meckel's cartilage (mk) was bifurcated (arrow) in the ectopic outgrowth and was surrounded by ectopic bone that was continuous with the dentary bone (db). Broken line demarcates the bifurcation of Meckel's cartilage. The end of the ectopic element (arrowhead) resembled the mandibular symphysis. (F) Sagittal section through the head of chimeric embryo 24 hours after transplantation demonstrates that in the mandible, *Shh* (yellow) and *Fgf8* (green) are normally expressed in adjacent domains in the oral ectoderm (arrows). By 24 hours after transplantation, *Shh* (yellow) and *Fgf8* (green) transcripts were still detected in the FEZ (asterisks), which was grafted to the aboral side of the mandible. Fnp, FNP; mx, maxillary process; fg, foregut. Scale bars: 2 mm in A-C; 1 mm in D,E; 0.5 mm in F.

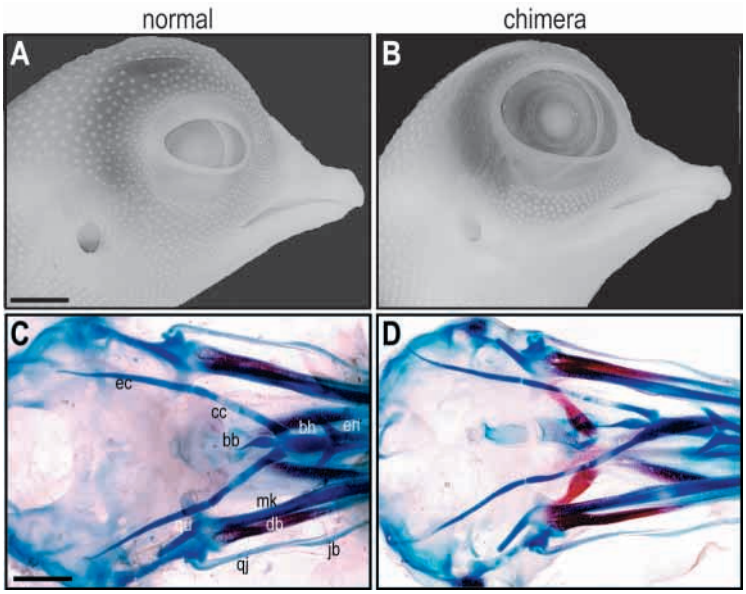

Fig. 7. The FEZ graft does not alter hyoid arch pattern. (A) Side and (C) ventral view of normal, unoperated, and (B,D) chimeric embryo 5 days after transplantation of the FEZ to the hyoid arch demonstrates that no ectopic growth was observed after this transplantation. (C) The proximal region of the hyoid arch comprises the epibranchial (ec) and ceratobranchial cartilages (cc), while the more distal region of the hyoid arch comprises the basihyal (bh), the basibranchial (bb) and the entoglsossum (en). (D) After transplantation, these elements appear normal. mk, Meckel's cartilage; db, dentary bone; qu, quadrate; qj, qudratojugal; jb, jugal bar. Scale bar: 2 mm.

placed (n=10; Fig. 8D). The upregulation of *Ptc1* and *Gli1* in the mesenchyme around the bead confirmed that the protein was bioactive (data not shown). Shh-N bead treatment caused an increase in the overall size of the distal upper beak including the premaxilla, but did not alter dorsoventral patterning (Fig. 8E,F). In a parallel series of experiments, we implanted Fgf2 beads underneath the dorsal FNP ectoderm (Fig. 8G). Although the protein was bioactive, as determined in a limb assay (data not shown), Fgf2 beads altered neither the overall size nor the dorsoventral pattern of the upper beak (n=12, Fig. 8H,I). Fgf2 and Shh-N beads in combination did not affect dorsoventral patterning of the FNP either (n=8; data not shown). Therefore, Shh-N and Fgf2 by themselves could not recapitulate the patterning effects of the FEZ.

DISCUSSION

The FEZ re-specifies the pattern of FNP and mandibular neural crest

Our experimental results indicate that a discrete region of facial ectoderm, which we refer to as the frontonasal ectodermal zone (FEZ), regulates proximodistal growth and dorsoventral patterning within the FNP. When grafted ectopically, the FEZ provokes a re-patterning of FNP and first pharyngeal arch mesenchyme, resulting in the duplication of FNP and mandibular skeletal elements.

The establishment of the FEZ begins prior to the arrival of FNP neural crest into the primordium. For example, *Fgf8* is restricted to dorsal FNP ectoderm; this expression domain is established at the time of neural tube closure (Marcucio et al., 2001). *Barx1* and *Pax6* are restricted to ventral FNP ectoderm; their expression domains are evident in this tissue long before neural crest cells are present in the FNP (R.S.M. and J.A.H., unpublished). Thus, the segmented characteristics of the FNP ectoderm develop independently of the presence of neural crest cells.

Our data indicate that stage 20 FNP ectoderm has the ability to re-specify facial pattern (Fig. 4); this patterning capacity is lost with time. Unpublished results from other investigators suggest that cephalic ectoderm from early neurulas does not exhibit any patterning activity (Couly et al., 2002). We interpret these seemingly paradoxical findings as an indication that the FEZ acquires the ability to specify FNP pattern sometime between the conclusion of neurulation and upon arrival of neural crest cells in the primordium. The acquisition of patterning ability over time is a feature shared by other organizing tissues, including the zone of polarizing activity in the limb bud (Wilson and Hinchliffe, 1985).

Recently, the pattern 'of every given bone in the face' has been proposed to be 'pre-featured' in pharyngeal endoderm (Couly et al., 2002). Although the endoderm clearly influences patterning of the first pharyngeal arch skeleton, it is improbable that this tissue contributes to patterning the skeletal derivatives of the FNP. Cranial neural crest destined for the FNP migrate over the forebrain rather than past the pharyngeal endoderm, making it unlikely that signals from this tissue impact neural crest skeletal precursors en route to the FNP. Once resident in the FNP, these same neural crest cells are sandwiched between neural ectoderm of the forebrain and facial ectoderm, rather than pharyngeal endoderm. Nonetheless, our data and those of others (Couly et al., 2002) indicate that epithelia provide instructive cues that direct patterning within neural crest-derived mesenchyme. This raises the obvious question of whether or not neural crest cells from different axial levels are equivalent in their ability to respond to such instructive cues.

Our data demonstrate that only a subset of neural crest cells can respond to patterning cues from the FEZ. Neural crest cells that originate rostral to rhombomere 3, which are devoid of Hox gene expression, respond to FEZ cues, whereas neural crest cells from rhombomere 4, which are Hox-positive, are unresponsive to FEZ cues. Pharyngeal endoderm exhibits the same ability to pattern Hox-negative, but not Hox-positive neural crest populations (Couly et al., 2002). Although these observations are in accordance with the theory that a Hox code establishes a type of pre-pattern within the pharyngeal skeleton (Gendron-Maguire et al., 1993; Kanzler et al., 1998; Rijli et al., 1993), they also leave open the possibility that neural crest of the frontonasal, maxillary and mandibular primordia are highly responsive to local patterning cues.

The FEZ directs dorsoventral patterning in the upper beak skeleton

Changing the dorsoventral orientation of the FEZ graft changes the dorsoventral orientation of the duplicated structures. Thus, FNP ectoderm not only produces cues that pattern FNP skeletal elements, it also dictates their orientation relative to the body axis. Based on our experimental results, we formulated a model

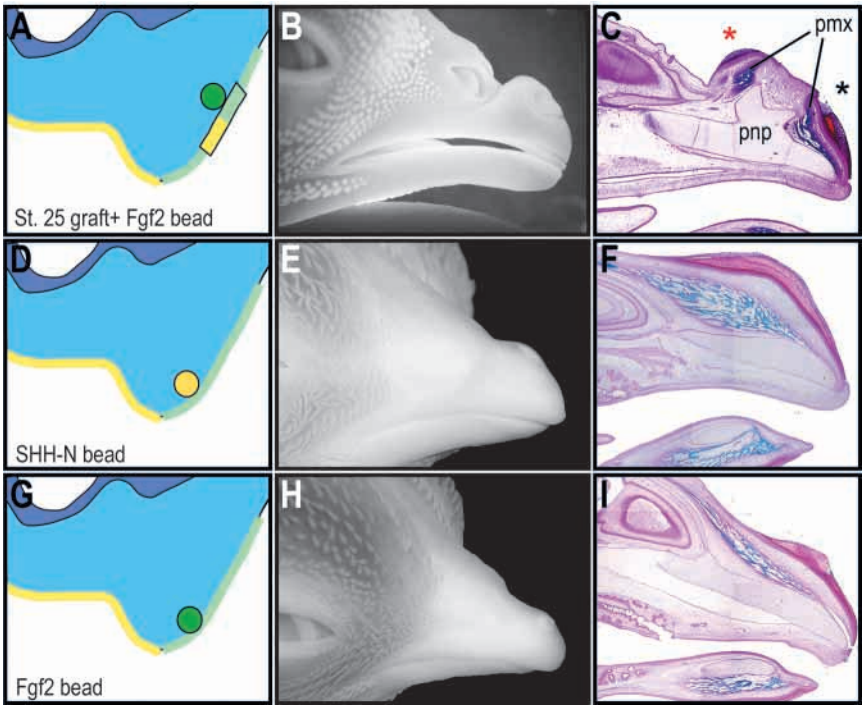

Fig. 8. Fgf2 can restore FEZ activity to stage 25 FNP ectoderm. (A) Schematic illustration of a stage 25 ectoderm graft combined with an Fgf2 bead (green circle). (B) Seven days later, the upper beak exhibited an abnormal shape. (C) Trichrome stained sections demonstrated the presence of a bifurcated prenasal process and premaxilla in the ectopic outgrowth, which indicated a DV polarity. (D) Schematic view illustrating the placement of a Shh-N bead (yellow circle) underneath the dorsal ectoderm of a stage 25 host. (E,F) Exogenous Shh-N resulted in an overall increase in size of the FNP skeletal elements, but no patterning alterations were observed. (G) Schematic illustrating placement of an Fgf2 bead beneath the dorsal ectoderm of a stage 25 FNP. (H,I) Exogenous Fgf2 had no discernible effect on FNP development.

whereby the juxtaposition of dorsal and ventral compartment boundaries specifies the dorsoventral pattern of the upper beak. This dorsoventral boundary model is predicated on the work of others.

One model, based primarily on the work of Mangold (Spemann and Mangold, 1924) and the work of Meinhardt (Meinhardt, 1983) proposes that the juxtaposition of differentially specified tissues leads to the generation of morphogen. An equally feasible hypothesis is that the juxtaposition of the same two tissues directly specifies cell fate (Lecuit and Cohen, 1997). In either scenario, cells located at the boundary itself can respond in unique ways to local cues because of their individual developmental histories. In the FNP, we propose that these differentially specified tissues are dorsal (e.g. *Fgf8*, *Bmp4* and *Wnt13* positive) and ventral (e.g. *Shh* and *Bmp2* positive) ectoderm. Interactions between the Fgf, Bmp, Wnt and Shh pathways are well documented during limb bud and neural tube development, and growing evidence indicates that these same pathways also interact in the FNP (Barlow and Francis-West, 1997; Duprez et al., 1996; Hu and Helms, 1999; Lee et al., 2001; Richman and Tickle, 1992; Schneider et al., 2001).

If we apply the principles of a boundary/organizer model to our experimental system, placing the graft into a dorsal compartment should result in an ectopic FEZ (contained within the graft itself) and the generation of at least one new intersection between ventral FEZ and dorsal host ectoderm (Fig. 5). The question is whether this new intersection acts as a FEZ. According to some boundary models, this intersection would be the site of morphogen production, which indirectly induces outgrowth. Our experimental data support this theoretical prediction (Fig. 4I,O; Fig. 5D). Our model also predicts that juxtaposing dorsal FEZ with dorsal host ectoderm would not result in an outgrowth; this is also our experimental observation (Fig. 5B). The ability of an epithelium to alter dorsoventral patterning in the face is not without precedence: pharyngeal endoderm can regulate the dorsoventral orientation of the first arch skeleton (Couly et al., 2002).

Epithelium or mesenchyme: which controls facial patterning?

Our data provide evidence that the instructive cues, which originate from a discrete region of FNP ectoderm, pattern FNP neural crest mesenchyme. The Hox-positive or Hox-negative status of the cells affects the interpretation of these ectodermal signals.

Our experimental results challenge the long-held belief that the neural crest is the source of patterning information in the face (reviewed by Chambers and McGonnell, 2002). In a number of developmental paradigms the ectoderm is responsible for directing morphogenesis of neural crest-derived tissues (Barlow et al., 1999; Hardcastle et al., 1999; Sarkar et al., 2000; Sarkar and Sharpe, 1999; Tucker et al., 1999). We show that local environmental cues can direct morphogenesis of the upper beak. In other experiments, we have recently shown that the particular response of the neural crest is based on species-specific characteristics (Schneider and Helms, 2003) and the rostrocaudal level from which the neural crest originates (Noden, 1983; Serbedzija et al., 1991).

In conclusion, the FEZ can direct outgrowth and dorsoventral pattern of the upper beak, but the precise shape of that upper beak undoubtedly depends upon patterning information inherent in the neural crest. Ultimately, the sculpting of a patterned tissue is the cumulative effect of stage-dependent reciprocal signaling events occurring between epithelia and mesenchyme. These experiments elucidate a new role for FNP ectoderm in regulating aspects of outgrowth and axis specification in the facial primordia.

The authors thank R. Schneider, D. Cordero, B. Eames and L. de la Fuente for critical reading and helpful discussions, D. Awai, C. Huang and K. H. Lee for technical assistance, and Cliff Tabin for providing cDNAs. They also thank Raymond F. Gariano for encouragement and inspiration. This work was supported by NIDCR K02 DE 00421 and R29 DE12462-03 to J.A.H., and is dedicated to Dr Carmelo Gariano.

REFERENCES

Albrecht, U. E. G., Helms, J. A. and Lin, H. (1997). Visualization of gene expression patterns by in situ hybridization. In *Molecular and Cellular Methods in Developmental Toxicology* (ed. G. P. Daston), pp. 23-48. Boca Raton, FL: CRC Press.

Artinger, K. B. and Bronner-Fraser, M. (1992). Partial restriction in the developmental potential of late emigrating avian neural crest cells. *Dev. Biol.* **149**, 149-157.

Baker, C. V., Bronner-Fraser, M., le Douarin, N. M. and Teillet, M. A. (1997). Early- and late-migrating cranial neural crest cell populations have equivalent developmental potential in vivo. *Development* **124**, 3077-3087.

Barlow, A. J., Bogardi, J. P., Ladher, R. and Francis-West, P. H. (1999). Expression of chick Barx-1 and its differential regulation by FGF-8 and BMP signaling in the maxillary primordia. *Dev. Dyn.* **214**, 291-302.

Barlow, A. J. and Francis-West, P. H. (1997). Ectopic application of recombinant BMP-2 and BMP-4 can change patterning of developing chick facial primordia. *Development* **124**, 391-398.

Bronner-Fraser, M. and Fraser, S. (1989). Developmental potential of avian trunk neural crest cells in situ. *Neuron* **3**, 755-766.

Chambers, D. and McGonnell, I. M. (2002). Neural crest: facing the facts of head development. *Trends Genet.* **18**, 381-384.

Couly, G., Creuzet, S., Bennaceur, S., Vincent, C. and le Douarin, N. M. (2002). Interactions between Hox-negative cephalic neural crest cells and the foregut endoderm in patterning the facial skeleton in the vertebrate head. *Development* **129**, 1061-1073.

Couly, G., Grapin-Botton, A., Coltey, P., Ruhin, B. and le Douarin, N. M. (1998). Determination of the identity of the derivatives of the cephalic neural crest: incompatibility between Hox gene expression and lower jaw development. *Development* **125**, 3445-3459.

Creuzet, S., Couly, G., Vincent, C. and le Douarin, N. M. (2002). Negative effect of Hox gene expression on the development of the neural crest-derived facial skeleton. *Development* **129**, 4301-4313.

Darwin, C. (1859). *The Origin of Species*. New York: The Crowell-Collier Publishing.

Dillon, R. and Othmer, H. G. (1999). A mathematical model for outgrowth and spatial patterning of the vertebrate limb bud. *J. Theor. Biol.* **197**, 295-330.

Dorsky, R. I., Moon, R. T. and Raible, D. W. (2000). Environmental signals and cell fate specification in premigratory neural crest. *BioEssays* **22**, 708-716.

Duprez, D. M., Kostakopoulou, K., Francis-West, P. H., Tickle, C. and Brickell, P. M. (1996). Activation of Fgf-4 and HoxD gene expression by BMP-2 expressing cells in the developing chick limb. *Development* **122**, 1821-1828.

Fekete, D. M. and Cepko, C. L. (1993). Replication-competent retroviral vectors encoding alkaline phosphatase reveal spatial restriction of viral gene expression/transduction in the chick embryo. *Mol. Cell Biol.* **13**, 2604-2613.

Gendron-Maguire, M., Mallo, M., Zhang, M. and Gridley, T. (1993). Hoxa-2 mutant mice exhibit homeotic transformation of skeletal elements derived from cranial neural crest. *Cell* **75**, 1317-1331.

Grammatopoulos, G. A., Bell, E., Toole, L., Lumsden, A. and Tucker, A. S. (2000). Homeotic transformation of branchial arch identity after Hoxa2 overexpression. *Development* **127**, 5355-5365.

Gurdon, J. B. and Bourillot, P. Y. (2001). Morphogen gradient interpretation. *Nature* **413**, 797-803.

Hamburger, V. and Hamilton, H. L. (1951). A series of normal stages in the development of the chick embryo. *J. Morphol.* **88**, 49-92.

Hardcastle, Z., Hui, C. C. and Sharpe, P. T. (1999). The Shh signalling pathway in early tooth development. *Cell. Mol. Biol.* **45**, 567-578.

Hu, D. and Helms, J. A. (1999). The role of sonic hedgehog in normal and abnormal craniofacial morphogenesis. *Development* **126**, 4873-4884.

Hunt, P., Clarke, J. D., Buxton, P., Ferretti, P. and Thorogood, P. (1998). Stability and plasticity of neural crest patterning and branchial arch Hox code after extensive cephalic crest rotation. *Dev. Biol.* **198**, 82-104.

Hunt, P., Whiting, J., Muchamore, I., Marshall, H. and Krumlauf, R. (1991a). Homeobox genes and models for patterning the hindbrain and branchial arches. *Development Suppl.* 187-196.

Hunt, P., Whiting, J., Nonchev, S., Sham, M. H., Marshall, H., Graham, A., Cook, M., Allemann, R., Rigby, P. W., Gulisano, M. et al. (1991b). The branchial Hox code and its implications for gene regulation, patterning of the nervous system and head evolution. *Development Suppl.* 63-77.

Hunt, P., Wilkinson, D. and Krumlauf, R. (1991c). Patterning the vertebrate head: murine Hox 2 genes mark distinct subpopulations of premigratory and migrating cranial neural crest. *Development* **112**, 43-50.

Kanzler, B., Kuschert, S. J., Liu, Y. H. and Mallo, M. (1998). Hoxa-2 restricts the chondrogenic domain and inhibits bone formation during development of the branchial area. *Development* **125**, 2587-2597.

Laufer, E., Nelson, C. E., Johnson, R. L., Morgan, B. A. and Tabin, C. (1994). Sonic hedgehog and Fgf-4 act through a signaling cascade and feedback loop to integrate growth and patterning of the developing limb bud. *Cell* **79**, 993-1003.

Lecuit, T. and Cohen, S. M. (1997). Proximal-distal axis formation in the Drosophila leg. *Nature* **388**, 139-145.

Lee, S. H., Fu, K. K., Hui, J. N. and Richman, J. M. (2001). Noggin and retinoic acid transform the identity of avian facial prominences. *Nature* **414**, 909-912.

Marcucio, R. S., Tong, M. and Helms, J. A. (2001). Establishment of distinct signaling centers in the avian frontonasal process. *Dev. Biol.* **235**, A432.

McGonnell, I. M., Clarke, J. D. and Tickle, C. (1998). Fate map of the developing chick face: analysis of expansion of facial primordia and establishment of the primary palate. *Dev. Dyn.* **212**, 102-118.

Meinhardt, H. (1983). A boundary model for pattern formation in vertebrate limbs. *J. Embryol. Exp. Morphol.* **76**, 115-137.

Meinhardt, H. (1984). Models for positional signalling, the threefold subdivision of segments and the pigmentation pattern of molluscs. *J. Embryol. Exp. Morphol. Suppl.* 289-311.

Noden, D. M. (1983). The role of the neural crest in patterning of avian cranial skeletal, connective, and muscle tissues. *Dev. Biol.* **96**, 144-165.

Presnell, J. K. and Schreibman, M. P. (1997). *Humason's Animal Tissue Techniques*. Baltimore, MD: The Johns Hopkins University Press.

Raible, D. W. and Eisen, J. S. (1996). Regulative interactions in zebrafish neural crest. *Development* **122**, 501-507.

Richardson, M. K. and Sieber-Blum, M. (1993). Pluripotent neural crest cells in the developing skin of the quail embryo. *Dev. Biol.* **157**, 348-358.

Richman, J. M. and Tickle, C. (1992). Epithelial-mesenchymal interactions in the outgrowth of limb buds and facial primordia in chick embryos. *Dev. Biol.* **154**, 299-308.

Rijli, F. M., Mark, M., Lakkaraju, S., Dierich, A., Dolle, P. and Chambon, P. (1993). A homeotic transformation is generated in the rostral branchial region of the head by disruption of *Hoxa-2*, which acts as a selector gene. *Cell* **75**, 1333-1349.

Sarkar, L., Cobourne, M., Naylor, S., Smalley, M., Dale, T. and Sharpe, P. T. (2000). Wnt/Shh interactions regulate ectodermal boundary formation during mammalian tooth development. *Proc. Natl. Acad. Sci. USA* **97**, 4520-4524.

Sarkar, L. and Sharpe, P. T. (1999). Expression of Wnt signalling pathway genes during tooth development. *Mech. Dev.* **85**, 197-200.

Schneider, R. A. (1999). Neural crest can form cartilages normally derived from mesoderm during development of the avian head skeleton. *Dev. Biol.* **208**, 441-455.

Schneider, R. A. and Helms, J. A. (2003). The cellular and molecular origin of beak morphology. *Science* **299**, 565-568.

Schneider, R. A., Hu, D., Rubenstein, J. L., Maden, M. and Helms, J. A. (2001). Local retinoid signaling coordinates forebrain and facial morphogenesis by maintaining FGF8 and SHH. *Development* **128**, 2755-2767.

Serbedzija, G. N., Burgan, S., Fraser, S. E. and Bronner-Fraser, M. (1991). Vital dye labelling demonstrates a sacral neural crest contribution to the enteric nervous system of chick and mouse embryos. *Development* **111**, 857-866.

Spemann, H. and Mangold, H. (1924). *Induction of Embryonic Primordia by Implantation of Organizers from a Different Species*. New York: Hafner.

Tucker, A. S., Al Khamis, A., Ferguson, C. A., Bach, I., Rosenfeld, M. G. and Sharpe, P. T. (1999). Conserved regulation of mesenchymal gene expression by Fgf-8 in face and limb development. *Development* **126**, 221-228.

Tyler, M. S. and Hall, B. K. (1977). Epithelial influences on skeletogenesis in the mandible of the embryonic chick. *Anat. Rec.* **188**, 229-240.

Wilson, D. J. and Hinchliffe, J. R. (1985). Experimental analysis of the role of the ZPA in the development of the wing buds of wingless (ws) mutant embryos. *J. Embryol. Exp. Morphol.* **85**, 271-283.

Wolpert, L. (1994). Positional information and pattern formation in development. *Dev. Genet.* **15**, 485-490.

Wolpert, L. (1996). One hundred years of positional information. *Trends Genet.* **12**, 359-364.

Ye, W., Shimamura, K., Rubenstein, J. L., Hynes, M. A. and Rosenthal, A. (1998). FGF and Shh signals control dopaminergic and serotonergic cell fate in the anterior neural plate. *Cell* **93**, 755-766.